High-efficiency, multicrystal, single-pass, continuous-wave second harmonic generation

S. Chaitanya Kumar,[1,*] G. K. Samanta,[1,2] Kavita Devi,[1] and M. Ebrahim-Zadeh[1,3]

[1]*ICFO-Institut de Ciencies Fotoniques, Mediterranean Technology Park, 08860 Castelldefels, Barcelona, Spain*
[2]*Currently at Physical Research Laboratory, Navarangpura, Ahmedabad 380 009, India*
[3]*Institucio Catalana de Recerca i Estudis Avancats (ICREA), Passeig Lluis Companys 23, Barcelona 08010, Spain*
**chaitanya.suddapalli@icfo.es*

Abstract: We describe the critical design parameters and present detailed experimental and theoretical studies for efficient, continuous-wave (cw), single-pass second harmonic generation (SHG) based on novel cascaded multicrystal scheme, providing >55% conversion efficiency and multiwatt output powers at 532 nm for a wide range of input fundamental powers at 1064 nm. Systematic characterization of the technique in single-crystal, double-crystal and multicrystal schemes has been performed and the results are compared. Optimization of vital parameters including focusing and phase-matching temperature at the output of each stage is investigated and strategies to achieve optimum SHG efficiency and power are discussed. Relevant theoretical calculations to estimate the effect of dispersion between the fundamental and the SH beam in air are also presented. The contributions of thermal effects on SHG efficiency roll-off have been studied from quasi-cw measurements. Using this multicrystal scheme, stable SH power with a peak-to-peak fluctuation better than 6.5% over more than 2 hours is achieved in high spatial beam quality with M^2<1.6.

OCIS codes: (190.2620) Harmonic generation and mixing; (190.4400) Nonlinear optics, materials; (140.7300) Visible lasers; (140.3510) Lasers, fiber.

References and links

1. J. Golden, "Green lasers score good marks in semiconductor material processing," Laser Focus World **28**, 75 (1992).
2. B. Hitz, "Green lasers gear up for display markets," Opt. Laser Europe **173**, 21–26 (2009).
3. R. J. Rockwell, Jr., "Designs and functions of laser systems for biomedical applications," Ann. N. Y. Acad. Sci. **168**, 459–471 (1969).
4. M. Tsunekane, N. Taguchi, and H. Inaba, "High-power, efficient, low-noise, continuous-wave all-solid-state Ti:sapphire laser," Opt. Lett. **21**(23), 1912–1914 (1996).
5. G. K. Samanta, G. R. Fayaz, and M. Ebrahim-Zadeh, "1.59 W, single-frequency, continuous-wave optical parametric oscillator based on MgO:sPPLT," Opt. Lett. **32**(17), 2623–2625 (2007).
6. L. McDonagh and R. Wallenstein, "Low-noise 62 W CW intracavity-doubled TEM_{00} Nd:YVO_4 green laser pumped at 888 nm," Opt. Lett. **32**(7), 802–804 (2007).
7. Z. Y. Ou, S. F. Pereira, E. S. Polzik, and H. J. Kimble, "85% efficiency for cw frequency doubling from 1.08 to 0.54, μm," Opt. Lett. **17**(9), 640–642 (1992).
8. R. Paschotta, P. Kürz, R. Henking, S. Schiller, and J. Mlynek, "82% Efficient continuous-wave frequency doubling of 1.06 μm with a monolithic MgO:$LiNbO_3$ resonator," Opt. Lett. **19**(17), 1325–1327 (1994).
9. A. Avramescu, T. Lermer, J. Müller, C. Eichler, G. Bruederl, M. Sabathil, S. Lutgen, and U. Strauss, "*S. Lutgen*, and *U. Strauss*, "True green laser diodes at 524 nm with 50 mW continuous wave output power on c-plane GaN," Appl. Phys. Express **3**(6), 061003–061006 (2010).
10. D. Heo, M. Park, J. Lee, and S. Hwang, S. Park and Y. Keh, "Optically pumped semiconductor laser," U.S. Patent 7474678 (Jan. 6, 2009)
11. U. Steegmueller, M. Kuehnelt, H. Unold, T. Schwarz, M. Schmitt, K. Auen, R. Schulz, C. Walter, I. Pietzonka, S. Illek, H. Lindberg, A. Gomez-Iglesias, M. Furitsch, C. Lauer, U. Strauss, and T. Hoefer, "Progress in ultra-compact green frequency doubled optically pumped surface emitting lasers," Proc. SPIE **7198**, 719807, 719807-8 (2009).
12. G. D. Miller, R. G. Batchko, W. M. Tulloch, D. R. Weise, M. M. Fejer, and R. L. Byer, "42%-efficient single-pass cw second-harmonic generation in periodically poled lithium niobate," Opt. Lett. **22**(24), 1834–1836 (1997).

#143851 - $15.00 USD Received 10 Mar 2011; revised 29 Apr 2011; accepted 17 May 2011; published 24 May 2011

13. G. K. Samanta, S. C. Kumar, M. Mathew, C. Canalias, V. Pasiskevicius, F. Laurell, and M. Ebrahim-Zadeh, "High-power, continuous-wave, second-harmonic generation at 532 nm in periodically poled KTiOPO(4).," Opt. Lett. **33**(24), 2955–2957 (2008).
14. M. Nakamura, S. Takekawa, K. Terabe, K. Kitamura, T. Usami, K. Nakamura, H. Ito, and Y. Furukawa, "Near-stoichiometric LiTaO 3 for bulk quasi-phase-matched devices," Ferroelectrics **273**(1), 199–204 (2002).
15. S. C. Kumar, G. K. Samanta, and M. Ebrahim-Zadeh, "High-power, single-frequency, continuous-wave second-harmonic-generation of ytterbium fiber laser in PPKTP and MgO:sPPLT," Opt. Express **17**(16), 13711–13726 (2009).
16. G. K. Samanta, S. C. Kumar, and M. Ebrahim-Zadeh, "Stable, 9.6 W, continuous-wave, single-frequency, fiber-based green source at 532 nm," Opt. Lett. **34**(10), 1561–1563 (2009).
17. G. K. Samanta, S. C. Kumar, R. Das, and M. Ebrahim-Zadeh, "Continuous-wave optical parametric oscillator pumped by a fiber laser green source at 532 nm," Opt. Lett. **34**(15), 2255–2257 (2009).
18. G. K. Samanta, S. Chaitanya Kumar, K. Devi, and M. Ebrahim-Zadeh, "Fiber-laser-pumped Ti:sapphire laser, " in *Conference on Lasers and Electro-Optics*, OSA Technical Digest (CD) (Optical Society of America, 2010), paper JTuD115.
19. I. Dolev, A. Ganany-Padowicz, O. Gayer, A. Arie, J. Mangin, and G. Gadret, "Linear and nonlinear optical properties of MgO:$LiTaO_3$," Appl. Phys. B **96**(2-3), 423–432 (2009).
20. S. Kumaragurubaran, S. Takekawa, M. Nakamura, and K. Kitamura, "Growth of 4-in diameter MgO-doped near-stoichiometric lithium tantalate single crystals and fabrication of periodically poled structures," J. Cryst. Growth **292**(2), 332–336 (2006).
21. S. Sinha, D. S. Hum, K. E. Urbanek, Y. Lee, M. J. F. Digonnet, M. M. Fejer, and R. L. Byer, "Room-temperature stable generation of 19 watts of single-frequency 532-nm radiation in a periodically poled lithium tantalate crystal," J. Lightwave Technol. **26**(24), 3866–3871 (2008).
22. N. E. Yu, S. Kurimura, Y. Nomura, and K. Kitamura, "Stable high-power green light generation with thermally conductive periodically poled stoichiometric lithium tantalate," Jpn. J. Appl. Phys. **43**(No. 10A), L1265–L1267 (2004).
23. A. Bruner, D. Eger, and S. Ruschin, "Second-harmonic generation of green light in periodically poled stoichiometric LiTaO3 doped with MgO," J. Appl. Phys. **96**(12), 7445–7449 (2004).
24. S. Spiekermann, F. Laurell, V. Pasiskevicius, H. Karlsson, and I. Freitag, "Optimizing non-resonant frequency conversion in periodically poled media," Appl. Phys. B **79**(2), 211–219 (2004).
25. T. Mizushima, H. Furuya, S. Shikii, K. Kusukame, K. Mizuuchi, and K. Yamamoto, "Second harmonic generation with high conversion efficiency and wide temperature tolerance by multi-pass scheme," Appl. Phys. Express **1**, 032003 (2008).
26. J. M. Yarborough, J. Falk, and C. B. Hitz, "Enhancement of optical second harmonic generation by utilizing the dispersion of air," Appl. Phys. Lett. **18**(3), 70–73 (1971).
27. G. C. Bhar, U. Chatterjee, and P. Datta, "Enhancement of second harmonic generation by double-pass configuration in barium borate," Appl. Phys. B **51**(5), 317–319 (1990).
28. G. Imeshev, M. Proctor, and M. M. Fejer, "Phase correction in double-pass quasi-phase-matched second-harmonic generation with a wedged crystal," Opt. Lett. **23**(3), 165–167 (1998).
29. S. V. Tovstonog, S. Kurimura, I. Suzuki, K. Takeno, S. Moriwaki, N. Ohmae, N. Mio, and T. Katagai, "Thermal effects in high-power CW second harmonic generation in Mg-doped stoichiometric lithium tantalate," Opt. Express **16**(15), 11294–11299 (2008).
30. D. Eimerl, "Quadrature frequency conversion," IEEE J. Quantum Electron. **23**(8), 1361–1371 (1987).
31. R. Thompson, M. Tu, D. Aveline, N. Lundblad, and L. Maleki, "High power single frequency 780nm laser source generated from frequency doubling of a seeded fiber amplifier in a cascade of PPLN crystals," Opt. Express **11**(14), 1709–1713 (2003).
32. G. K. Samanta, S. C. Kumar, K. Devi, and M. Ebrahim-Zadeh, "Multicrystal, continuous-wave, single-pass second-harmonic generation with 56% efficiency," Opt. Lett. **35**(20), 3513–3515 (2010).
33. M. M. Fejer, G. A. Magel, D. H. Jundt, and R. L. Byer, "Quasi-phase-matched second harmonic generation: Tuning and tolerances," IEEE J. Quantum Electron. **28**(11), 2631–2654 (1992).
34. A. Bruner, D. Eger, M. B. Oron, P. Blau, M. Katz, and S. Ruschin, "Temperature-dependent Sellmeier equation for the refractive index of stoichiometric lithium tantalate," Opt. Lett. **28**(3), 194–196 (2003).
35. D. S. Hum and M. M. Fejer, "Quasi-phasematching," C. R. Phys. **8**(2), 180–198 (2007).
36. G. D. Boyd and D. A. Kleinman, "Parametric interaction of focused Gaussian light beams," J. Appl. Phys. **39**(8), 3597–3639 (1968).
37. J. A. Armstrong, N. Bloembergen, J. Ducuing, and P. S. Pershan, "Interactions between light waves in a nonlinear dielectric," Phys. Rev. **127**(6), 1918–1939 (1962).
38. M. Abramowitz and I. Stegun, *Handbook of Mathematical Functions* (Dover, New York, 1965)
39. R. C. Eckardt and J. Reintjes, "Phase matching limitations of high efficiency second harmonic generation," IEEE J. Quantum Electron. **20**(10), 1178–1187 (1984).
40. D. Eimerl, "High average power harmonic generation," IEEE J. Quantum Electron. **23**(5), 575–592 (1987).

1. Introduction

High-power, continuous-wave (cw) green sources have demonstrated their potential in a wide range of applications, from material processing [1], display technology [2] and biomedicine [3], pumping of Ti:sapphire lasers [4] and cw optical parametric oscillators (OPOs) [5]. For

#143851 - $15.00 USD Received 10 Mar 2011; revised 29 Apr 2011; accepted 17 May 2011; published 24 May 2011

many of these applications, output power, stability, and beam quality are critical requirements. In the absence of suitable laser gain materials for the green spectral range, nonlinear optical techniques, in particular second harmonic generation (SHG) of 1-μm solid-state lasers, have been established as the most viable approach to provide green radiation. In cw regime, however, the attainment of high SHG conversion efficiencies is challenging, due to the low available nonlinear gain. To overcome this limitation, various techniques have been deployed to achieve practical cw SHG efficiency and output power. The most viable methods have relied on intracavity or external resonant enhancement in combination with birefringent nonlinear crystals. Using a 20-mm-long LBO crystal internal to a diode-pumped solid state laser, cw green powers of up to 62 W have been obtained at 532 nm, with diode-to-green optical conversion efficiency of 52% [6]. By deploying external enhancement in a 10-mm-long KTP crystal, a cw green power of 560 mW was obtained at 540 nm with a SHG efficiency of 85% [7], while the use of a monolithic enhancement resonator based on a 7.5-mm-long MgO:$LiNbO_3$ crystal resulted in the generation of 130 mW of 532 nm radiation at 82% conversion efficiency [8]. While internal and external enhancement techniques have been effective in the attainment of practical cw SHG powers and efficiencies, such approaches generally suffer from elaborate system designs involving intricate cavity configurations for internal doubling. Moreover, high sensitivity to thermal effects, or the need for active stabilization of external cavities, with the concomitant requirements of specialist mirrors for impedance matching and low-loss, damage-resistant crystal coatings, result in increased complexity and cost. Alternative routes to the generation of cw green radiation based on semiconductor lasers are also evolving. However, while diode lasers are available in some regions of the visible spectrum, such as blue and red, direct generation in the green has not been achieved until very recently [9], and much is yet to be done to attain practical powers in good beam quality. Optically pumped semiconductor lasers [10] offer another promising technology for cw green generation, but this approach also requires the use of nonlinear frequency conversion techniques [11].

An attractive alternative technique, which offers great simplicity and reduced cost, is external single-pass SHG (SP-SHG) of cw 1-μm lasers in quasi-phase-matched (QPM) ferroelectric crystals. Vital in the attainment of practical powers and efficiencies in this scheme is the ability to exploit long interaction lengths under noncritical phase-matching (NCPM) and the highest nonlinear coefficient accessible in QPM materials. Among the QPM ferroelectric crystals, periodically-poled $LiNbO_3$ (PPLN) has been most widely established for nonlinear frequency conversion applications, due to a mature fabrication technology, large effective nonlinearity (d_{eff}~16 pm/V), and widespread availability in interaction lengths up to 80 mm. Its use in cw SP-SHG has been previously demonstrated, where 2.7 W of green power has been generated with a 53-mm-long crystal for a fundamental power of 6.5 W at an internal conversion efficiency of 42% [12]. However, the potential of PPLN for visible generation remains constrained by photorefractive damage. Doping with MgO increases this damage threshold, but stable generation of visible and green radiation is still increasingly problematic at higher optical powers. An alternative QPM material candidate for cw green generation is periodically-poled $KTiOPO_4$ (PPKTP), offering moderate effective nonlinear coefficient (d_{eff}~10pm/V). However, despite its wide temperature acceptance bandwidth, low thermal conductivity makes it more sensitive to thermal effects, limiting its use at higher powers [13]. Periodically-poled $LiTaO_3$ (PPLT) is an attractive alternative material, which possesses an effective nonlinear coefficient comparable to PPKTP (d_{eff}~9 pm/V), but with higher thermal conductivity. On the other hand, as a member of $LiNbO_3$ family of ferroelectrics, PPLT also requires high coercive field (~21 kV/mm) for poling and suffers from photorefractive damage. However, with stoichiometric composition (PPsLT), the coercive field can be dramatically reduced, and doping with MgO (MgO:sPPLT) can also increase the photorefractive damage threshold by as much as three orders of magnitude, further reducing the coercive field [14]. Our recent studies have shown that MgO:sPPLT is a promising candidate for cw SP-SHG [15,16], owing to its superior thermal and optical properties, as summarized in Table 1. Using a 30-mm-long MgO:sPPLT crystal and a cw Yb fiber laser, we achieved a cw SP-SHG

#143851 - $15.00 USD Received 10 Mar 2011; revised 29 Apr 2011; accepted 17 May 2011; published 24 May 2011

conversion efficiency of 32.7%, providing 9.6 W of green power for 29.5 W a fundamental power [16]. We also successfully used this green fiber source to pump a cw OPO [17] and a Ti:sapphire laser [18]. With the rapid continuing advances in cw fiber lasers offering unprecedented optical powers near 1 μm, this approach also offers increasing potential for the realization of compact, high-power cw green sources in simplified, cost-effective, and practical designs.

Table 1. Optical and thermal properties of MgO:sPPLT

Transmission range (μm)	0.2–6	[19]
Maximum available crystal length (mm)	40	[20]
Maximum available crystal thickness (mm)	3	[14,20]
Effective nonlinear coefficient (pm/V)	~9	[19]
Coercive field (kV/mm)	1.4	[14]
Absorption at 1064 nm (%/cm)	0.17	[15]
Absorption at 532 nm (%/cm)	1.57	[15]
Green induced absorption at 1064 nm (cm/GW)	5	[21]
Thermal conductivity (W/m-K)	8.4 (0.5% Mg)	[22]
Photorefractive damage threshold (MW/cm^2)	>2	[23]
Surface damage threshold (GW/cm^2)	0.57	[22]

2. Single-pass cw SHG

The most direct strategy for the attainment of highest conversion efficiency and output power in cw SP-SHG is to maximize nonlinear gain by deploying the longest available crystal length for any given fundamental power. While, in principle, restrictions imposed by temperature, spectral and angular acceptance for phase-matching can limit the maximum usable interaction length, in practice the maximum usable length is limited by crystal growth and fabrication technology for QPM materials (30-40 mm in MgO:sPPLT). Therefore, given the limited available interaction lengths, it is necessary to devise viable strategies to achieve practical powers and conversion efficiencies in cw SP-SHG at any fundamental power.

At low to moderate fundamental powers (<10 Watts), where cw SP-SHG efficiency is hampered by low nonlinear gain, the use of the longest crystal length is imperative to obtain practical output power. To enhance efficiency and power, schemes such as double-pass and multi-pass pumping may be deployed [24,25] to increase the effective interaction length. However, successful exploitation of such techniques requires accurate control of relative phase in successive passes through the crystal to compensate for phase-mismatch, using dispersion in air [26,27] or wedged crystals [28]. These schemes also require optical isolation to protect the pump laser from back-reflected undepleted pump. Additionally, multi-pass pumping gives rise to crystal heating effects at even moderate pump powers, due to the increased pump and SH intensities, resulting from the periodic refocusing of the undepleted pump at the center of the crystal. This can lead to increased thermal dephasing or lensing, thus degrading efficiency and output beam quality. Moreover, the higher focused local intensity of fundamental and second harmonic in the same crystal can increase material damage risk. In addition, since the acceptance bandwidths for phase-matching scale inversely with the number of passes, such schemes can also lead to narrowing of the overall acceptance bandwidth and thus a reduction in gain [24]. The restriction on the longest available QPM crystal length and the constraints of double-pass and multi-pass schemes thus set a limit to the maximum attainable efficiency and output power in cw SHG at low to moderate powers, thus requiring alternative strategies.

At higher pump powers (>10 W), shorter interaction lengths can be tolerated, while providing practical cw powers at reduced efficiency. By deploying a fundamental power as high as 100 W, a cw SP-SHG efficiency of 17.6% has been obtained in a MgO:sPPLT crystal as short as 10 mm [29]. However, attempts to increase cw SP-SHG efficiency using longer

#143851 - $15.00 USD Received 10 Mar 2011; revised 29 Apr 2011; accepted 17 May 2011; published 24 May 2011

crystals can be hampered by increasing thermal effects. Thermal phase-mismatch can result from crystal heating at higher powers due to residual absorption, and becomes more important with increase in length, diminishing nonlinear gain and efficiency, and thus inhibiting power scaling. Moreover, it becomes increasingly difficult to maintain a constant phase-matching temperature over the entire length of a long crystal, particularly at higher powers, leading to further thermal dephasing and thus reducing the effective interaction length. In MgO:sPPLT, thermal dephasing arises from the residual absorption of fundamental as well as a higher contribution from the green absorption to crystal heating [15]. Thermal lensing due to residual absorption cannot be ruled out at high pump powers, resulting in degradation in output beam quality. The use of double-pass or multi-pass pumping is also not as desirable at high pump powers as may be entertained at low powers, because of the increased risk of damage and thermal effects. To minimize such risks, multiple single-pass pumping in a 25-mm-long, wide-aperture MgO:PPLN crystal has been used, resulting in a cw SHG efficiency of 66% [25], but the resulting poor quality of the output beam limits the effectiveness of this approach. As such, enhancement of cw SHG conversion efficiency by deploying multi-pass configurations requires careful optimization and proper engineering of the nonlinear crystal [24].

It is thus clear that while SP-SHG remains the most direct, simple, compact, and practical approach for the generation of cw green radiation, attainment of high conversion efficiency and output power requires the deployment of alternative new techniques. Here we describe a novel implementation for cw SP-SHG based on a cascaded multicrystal scheme, which can provide the highest conversion efficiency at any given fundamental power, while overcoming the limitations of other approaches deployed to date. The use of multiple nonlinear crystals is a potentially attractive approach to achieve increased cw SP-SHG efficiency and power. Such a scheme based on birefringent phase-matching was extensively studied for SP-SHG of pulsed laser radiation and resulted in the development of quadrature frequency conversion [30], but this method leads to transversely varying polarization in the generated SH beam. The use of two QPM nonlinear crystals has also been investigated in the cw regime [31]. By deploying two 50-mm-long PPLN crystals, 900 mW of tunable cw radiation near 780 nm was generated for a fundamental power of 4.8 W, at an overall SP-SHG efficiency of ~19%, with a normalized efficiency of 5.6 mW/W^2-cm (2.8%/W). This performance was achieved by confocal refocusing of the undepleted fundamental power from the first crystal into the second crystal using a lens, which can result in increased phase-mismatch effects, and thus reductions in conversion efficiency. Recently, using a novel multicrystal scheme based on three identical 30-mm-long MgO:sPPLT crystals in a cascade, we demonstrated SP-SHG of a cw Yb fiber laser with a conversion efficiency as high as 56%, in the low- to moderate-power as well as high-power regime, providing as much as 5.6 W of green output for 10 W and 13 W green output for 25.1 W of input pump power [32]. This performance was made possible by refocusing both fundamental and SH beams into the successive crystals using concave mirrors of suitable radius of curvature, thereby avoiding phase retardation between the beams in passing through refractive lens media, by the ability to achieve perfect and independent mode matching in consecutive crystals, and through the control of fundamental depletion and conversion in each stage to achieve the highest overall cw SP-SHG efficiency and output power. Although this technique is very simple, the optimization of such a cascaded scheme is not trivial. Various crucial parameters including the phase-matching temperature and the pump depletion in each stage have to be carefully controlled to achieve the highest overall output SHG efficiency. Such details about the cascaded approach using multiple nonlinear crystals have not been previously discussed in our earlier work [32] or, to our knowledge, by other researchers. Hence, a comprehensive study of the multicrystal SP-SHG scheme is timely and of considerable importance.

In this report, we present a rigorous study of cw SP-SHG using multiple nonlinear crystals in cascade, and compare the performance characteristics with regard to the most important parameters including SHG power and efficiency, from single-crystal to multicrystal scheme. The optimization of various critical parameters including mode-matching and focusing, phase-

#143851 - $15.00 USD Received 10 Mar 2011; revised 29 Apr 2011; accepted 17 May 2011; published 24 May 2011

matching temperature and pump depletion at the output of each individual stage to maximize SHG efficiency is discussed in detail. Also, the effect of crystal housing configuration on SHG efficiency is studied. Using this technique, we demonstrate an increase in cw SP-SHG efficiency by ~4 times from the single-crystal (SC) to double-crystal (DC) scheme in the high-power regime, providing 13 W of green power at an overall efficiency of 51.8% for 25.1 W of fundamental power. Using multicrystal (MC) scheme involving three crystals, we further enhance the cw SP-SHG efficiency by ~8 times in the low- to moderate-power regime compared to SC scheme, generating 5.6 W of green power for 10 W of fundamental power at an overall efficiency as high as 56% [32]. Relevant theoretical calculations are presented to estimate the effect of dispersion between the fundamental and the SH beam, while traversing between the successive stages in the MC scheme. The quasi-cw measurements illuminate the role of thermal effects and SHG efficiency roll-off, which such systems involving high optical powers are known to exhibit. To our knowledge, the conversion efficiency of 56% is the highest in cw SP-SHG achieved to date, using bulk QPM or birefringent nonlinear crystals. Moreover, the described technique is generic, and can be extended to more than three crystals in a cascade to achieve the highest overall cw SP-SHG efficiency and output power for any given input fundamental power. Combined with the rapid advances in cw Yb fiber lasers, the approach offers a highly effective route for the realization of simplified, compact, efficient, and cost-effective green sources from a few watts to several watts of output power.

2.1 Theory

An important factor in the attainment of the highest cw SP-SHG efficiency is to deploy the longest interaction length available. However, within the restrictions imposed by QPM material growth and fabrication technology, considerations of spectral, temperature and angular acceptance bandwidth are necessary to determine the optimum crystal length for maximum SHG conversion efficiency [33]. In the case of MgO:sPPLT used in the present work, crystal lengths up to 30 mm are commercially available. The acceptance bandwidths for a 30-mm-long MgO:sPPLT crystal are shown in Fig. 1. Using the Sellmeier equation for the

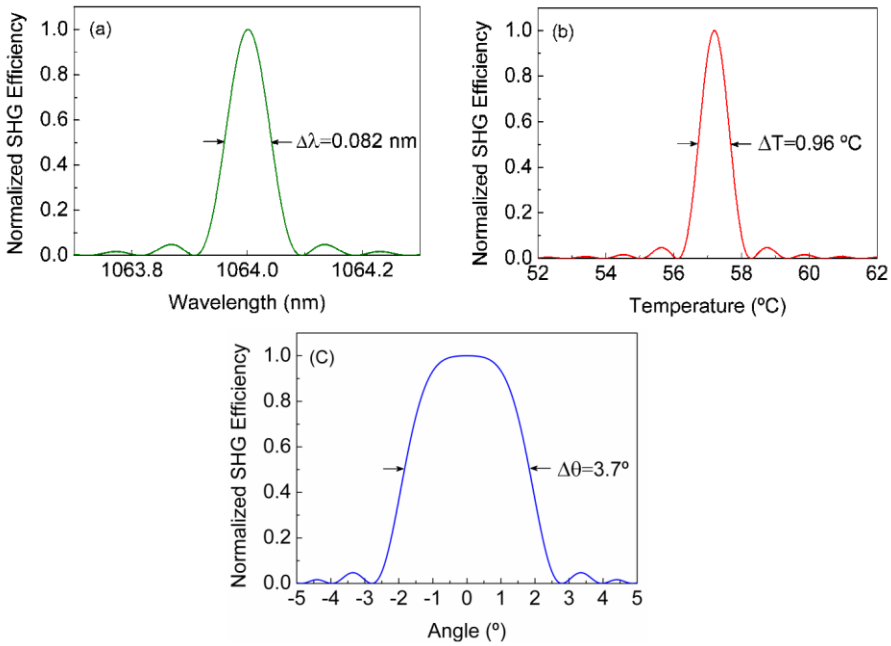

Fig. 1. (a) Spectral, (b) temperature, and (c) angular acceptance bandwidth of 30-mm-long MgO:sPPLT nonlinear crystal.

#143851 - $15.00 USD Received 10 Mar 2011; revised 29 Apr 2011; accepted 17 May 2011; published 24 May 2011

material [34], the spectral, temperature and angular acceptance bandwidths are calculated to be $\Delta\lambda = 0.082$ nm, $\Delta T = 0.96$ °C [15,16] and $\Delta\theta = 3.7°$, respectively.

The generated second harmonic power is a quantity of more practical importance, and SHG conversion efficiency in plane wave approximation, with no depletion of the fundamental wave, is given by [35]

$$\eta = \frac{P_{2\omega}(L)}{P_{\omega}(0)} = \eta_{norm}\left[\frac{P_{\omega}L^2}{A}\right]\sin c^2\left(\frac{\Delta KL}{2}\right), \qquad \eta_{norm} = \frac{8\pi^2 d_{eff}^2}{n_{\omega}^2 n_{2\omega} c\varepsilon_0 \lambda_{\omega}^2} \tag{1}$$

In case of focused Gaussian beams, this expression needs to be modified, and the SHG efficiency is given by [35]

$$\eta = \frac{16\pi^2 d_{eff}^2 h}{n_{\omega} n_{2\omega} c\varepsilon_0 \lambda_{\omega}^3} LP_{\omega}, \qquad \Delta K = K_{2\omega} - K_{\omega} - \frac{2\pi}{\Lambda} \tag{2}$$

where η_{norm} is the normalized SHG conversion efficiency, d_{eff} is the effective nonlinear coefficient, h is the Boyd and Kleinman focusing parameter [36], n_{ω} and $n_{2\omega}$ are the refractive indices at the fundamental and SH wavelengths, respectively, c is the velocity of light, ε_0 is the permittivity of free space, λ_{ω} is the fundamental wavelength, L is the length of the nonlinear crystal, ΔK is the QPM wave-vector mismatch and Λ is the QPM grating period.

The SHG of a monochromatic plane wave can be understood by solving the coupled-wave equations. Armstrong *et al.* have derived and solved these equations for SHG. The exact solution of the coupled-wave equations with zero input at the SH wavelength is given by [37]

$$\eta = V_b^2 sn^2\left(\frac{\Gamma L}{V_b}\middle| V_b^4\right), \quad V_b = \left[\frac{\Delta S}{4} + \sqrt{1+\left(\frac{\Delta S}{4}\right)^2}\right]^{-1}, \quad \Delta S = \frac{\Delta K}{\Gamma}, \quad \Gamma = \sqrt{\eta_{norm} I_{\omega}} \tag{3}$$

where *sn* is a Jacobi elliptic function [38]. In the limit of no fundamental wave depletion, Eqs. (3) simplify to Eqs. (1), while in case of perfect phase-matching with fundamental wave depletion, Eqs. (3) become [37,39]

$$\eta = \tanh^2(\Gamma L) \tag{4}$$

Efficient SHG involving high fundamental and second harmonic power leads to thermal dephasing effects due to the absorption in the nonlinear crystal. This effect of thermal dephasing ($\delta = \Delta KL/2$), on the SHG efficiency, as a function of the nonlinear drive ($\eta_0 = \Gamma^2 L^2$), has been considered by Eimerl [40]. He pointed out that, for efficient conversion, the total dephasing (δ) must be less than $\pi/10$, which is fortunately possible with QPM using low nonlinear drive.

All above expressions have been derived by assuming no SH signal at the input to the nonlinear crystal. However, in the present experiment, where multiple nonlinear crystals are deployed to enhance the SHG efficiency in single-pass configuration, the nonlinear crystals

#143851 - $15.00 USD Received 10 Mar 2011; revised 29 Apr 2011; accepted 17 May 2011; published 24 May 2011

after the first have non-zero input at the second harmonic wavelength. The SHG efficiency in such a case, with optimum relative phase of $\phi_{2\omega}$-$2\phi_{\omega} = \pm \pi/2$ between the fundamental and SH wave at the input, and under perfect phase-matching, becomes [37]

$$\eta = \tanh^2\left(\Gamma(l_0 + L)\right) \tag{5}$$

The effect of non-zero input at the SH wavelength can be thus be considered as an increase in the length of the nonlinear crystal by a value, l_0. Hence, two individual 30-mm-long crystals can be considered as single crystal of 60-mm length. Figure 2 shows the SHG efficiency as a function of incident fundamental power for MgO:sPPLT nonlinear crystals of length 30 mm, 60 mm and 90 mm, as calculated from Eqs. (3). It is to be noted that thermal dephasing effects and back-conversion are not considered in this calculation. The estimated fundamental power required to achieve a SHG efficiency of 55% in single-pass configuration is 17.8 W and 12 W in MgO:sPPLT crystals of length 60 mm and 90 mm, respectively, while a fundamental power greater than 30 W is needed to achieve a similar SH efficiency using a 30 mm-long crystal. With these estimates of the required fundamental power, we deployed the novel multicrystal cw SP-SHG scheme to achieve the highest conversion efficiencies, with the results of these experiments described below.

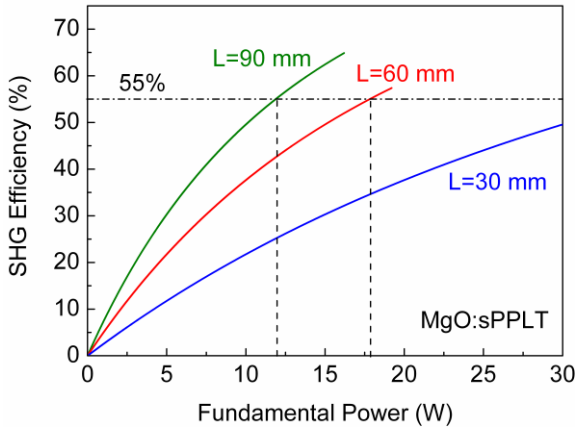

Fig. 2. Theoretically calculated SHG efficiency for different lengths of the MgO:sPPLT nonlinear crystal as a function of fundamental power.

2.2 Experimental setup

The schematic of experimental configuration for the MC cw SP-SHG experiments is shown in Fig. 3. The fundamental pump source is a cw Yb fiber laser (IPG Photonics, YLR-30-1064-LP-SF) delivering linearly polarized single-frequency radiation at 1064 nm with a maximum output power of 30 W and a nominal linewidth of 89 kHz. An isolator at the output end of the fiber protects the laser from any back-reflections. Using a lens of f = 25 cm focal length and a scanning beam profiler, we measured the laser to have a beam quality factor M^2<1.01. In order to maintain stable output characteristics, the fiber laser is operated at maximum power and the input power to the SHG crystal is adjusted by using a combination of half-wave plate and polarizing beam-splitter cube. A second half-wave plate is used to obtain the correct polarization for phase-matched SHG in the nonlinear crystal. We use three identical MgO:sPPLT crystals, each 30-mm-long, 2-mm-wide and 1-mm-thick, and containing a single grating period of Λ = 7.97 μm. The end faces of all three crystals are antireflection-coated (R<1%) at 1064 nm and 532 nm. Each crystal is housed in a separate oven with temperature stability better than ± 0.1 °C. Our earlier studies on nonlinear crystal housing configurations has revealed that a significant improvement in the SHG efficiency can be obtained by proper design of the mount for the crystal, to provide efficient thermal management [15]. Using two different oven designs for the crystal, we have found a significant difference in the generated

#143851 - $15.00 USD Received 10 Mar 2011; revised 29 Apr 2011; accepted 17 May 2011; published 24 May 2011

green power and cw SP-SHG conversion efficiency between the two configurations. The two crystal housing configurations, open-top (OT) and close-top (CT), are shown in Fig. 4. The OT configuration resulted in better performance, due to the easier exchange of heat between the nonlinear crystal and the ambient air, permitting the optimum phase-matching to be achieved and maintained. The MC SP-SHG setup consists of three stages. In stage-1, the fundamental beam is focused into the nonlinear crystal using a lens of focal length f = 175 mm, resulting in a beam waist radius of ω_1~31 μm, positioned at the center of the crystal. In stage-2, the generated SH and undepleted fundamental from stage-1 are collimated using a plano-concave mirror, M_1, and refocused into the second crystal using M_2. The SH thus generated, and the un-depleted fundamental are again collimated and refocused by using plano-concave mirrors, M_3 and M_4, into the third crystal in stage-3. The radius of curvature (ROC) of all mirrors, M_1-M_4, are chosen according to the required beam waist for mode-matching at the center of each crystal. The angle of incidence on each mirror is limited by the mechanical constraints and kept as small as possible. All plano-concave mirrors are coated for high reflectivity (R > 99%) at 1064 nm and 532 nm, and are mounted on translation stages, so as to adjust the inter-crystal spacing, to compensate for the accumulated phase due to dispersion in air, if there is any. A plane dichroic mirror, M, coated for high reflectivity (R > 99%) at 532 nm and high transmission (T > 99%) at 1064 nm, is used to extract the generated green output from the fundamental. Unlike lenses [31], using plano-concave mirrors to collimate and refocus the beams into the successive stages, avoids any additional phase retardation issues between the fundamental and SH wavelengths due to material dispersion.

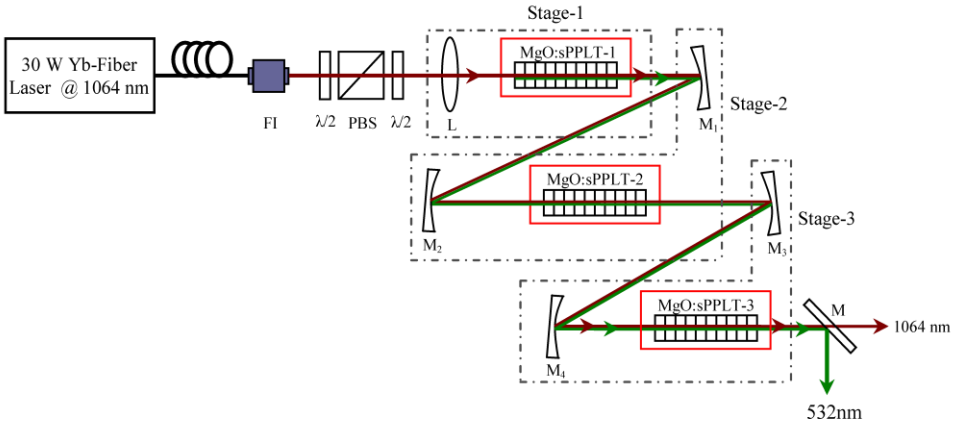

Fig. 3. Experimental setup for the multicrystal cw single-pass SHG

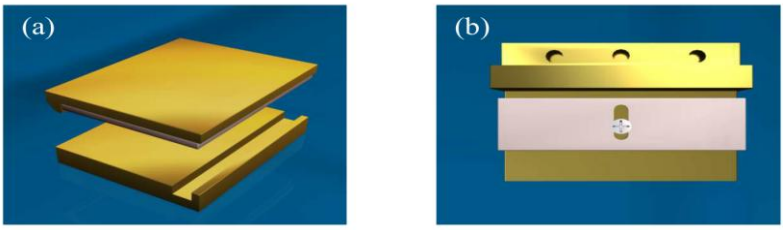

Fig. 4. (a) Close-top (CT), and (b) Open-top (OT) crystal housing configurations used for MgO:sPPLT in the multicrystal cw single-pass SHG experiments.

In order to achieve efficient SHG, we systematically characterized the setup in DC and then in MC schemes and the results thus obtained are compared to evaluate the performance.

#143851 - $15.00 USD Received 10 Mar 2011; revised 29 Apr 2011; accepted 17 May 2011; published 24 May 2011

2.3 Single-crystal cw single-pass SHG

A complete characterization of cw SP-SHG in SC scheme based on MgO:sPPLT was performed in our earlier work, where the temperature phase-matching properties were studied in detail [15,16]. The SC cw SHG was characterized by focusing the fundamental beam to a waist radius of ω_1~30 µm inside a 30-mm-long MgO:sPPLT crystal housed in an oven in CT configuration. The temperature acceptance bandwidth was measured to be 1.3 °C, centered at a phase-matching temperature of 52 °C. Using a single MgO:sPPLT crystal in the CT oven configuration, we generated 7.8 W of green for a fundamental power of 29.5 W at a cw SP-SHG efficiency of 26.4%, while by employing the OT design, we were able to increase the green power to 9.6 W at 32.7% conversion efficiency for the same input fundamental power.

2.4 Double-crystal cw single-pass SHG

The DC cw SP-SHG setup is characterized by focusing the SH green and the undepleted fundamental from stage-1 into the second identical MgO:sPPLT crystal by a proper choice of M_1 and M_2. The net physical length of the nonlinear crystal in DC scheme is 60 mm (2 x 30 mm). The second crystal is initially mounted in CT housing configuration. In order to scale the SHG efficiency, ROC of M_1 and M_2 are chosen to be r = 150 mm, such that a mirror image of the beam waist in the first crystal is formed at the center of the second crystal, resulting in a beam waist radius of ω_2~30 µm. The fundamental power is measured before stage-1 and the SH power is measured after stage-2 for scaling. The SHG efficiency scaling results under this focusing condition are shown in Fig. 5(a). The SHG efficiency increases linearly up to a fundamental power of 7 W, above which saturation behavior is observed. A maximum efficiency of 48.5% is achieved at fundamental power of 20.4 W. Further increase in the fundamental power resulted in catastrophic damage of the second crystal. The origin of this damage could be attributed to the strong focusing of both the fundamental as well as the SH beam, or poor quality of the crystal sample used in stage-2. Further experiments are needed to understand this damage phenomenon in detail. In order to avoid the damage, we replaced M_2 with another mirror of r = 250 mm, resulting in beam waist radius of ω_2~46 µm at the center of the second crystal and performed SHG efficiency scaling measurements, the results of which are also shown in Fig. 5(a). The stage-2 is maintained at a distance of ~37 cm from the stage-1. The SHG efficiency in case of ω_2~46 µm follows that at ω_2~30 µm, very closely at low fundamental power level. Although saturation is observed under both focusing conditions, the maximum achievable SHG efficiency increased to 50.7% for a fundamental power of 18.4 W at the input of stage-1. To investigate the role of crystal mounting configurations, we performed SHG power and efficiency scaling measurements in the OT design for the same beam waist of ω_2~46 µm in the second crystal, with the results shown in Fig. 5(b). Using the OT configuration, maximum SHG efficiency as high as 54.8% is achieved with a SH power of 11.6 W for a fundamental power of 21.1 W, confirming the

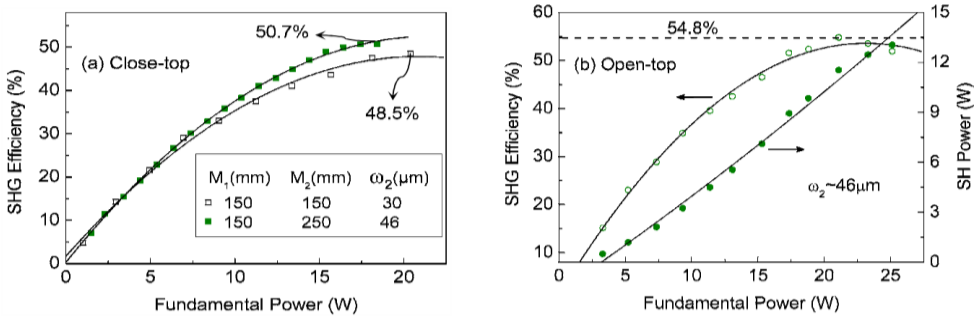

Fig. 5. (a) Variation of SHG efficiency as function of fundamental power for a beam waist radius of ω_2~30 µm and 46µm in CT configuration, (b) SH Power and efficiency scaling for a beam waist radius of ω_2~46µm in OT configuration.

#143851 - $15.00 USD Received 10 Mar 2011; revised 29 Apr 2011; accepted 17 May 2011; published 24 May 2011

better performance of OT configuration. It is also to be noted that we were able to use an input fundamental power greater than 20 W without any catastrophic damage to the second crystal, generating as much as 13 W of green power for a fundamental power of 25.1W. However, the SHG efficiency roll-off occurs when the fundamental power increased above 21.1 W. Having achieved SHG efficiency as high as 54.8% in the DC scheme, we extend this technique to one more stage, by deploying a third crystal in the cascade, to further increase the SHG efficiency and power.

2.5 Multicrystal cw single-pass SHG

The MC cw SP-SHG scheme is realized by focusing the SH green as well as the undepleted fundamental from the output of the DC scheme into a third crystal by using another pair of plano-concave mirrors, M_3 and M_4. The net physical length of the nonlinear crystal in the MC scheme is 90 mm (3 x 30 mm). Efficient mode-matching, proper choice of the confocal focusing parameter, and careful control of the pump depletion, enables the exploitation of the maximum effective interaction length to achieve highest SHG efficiency. The ROC of M_3 and M_4 are chosen to be r = 150 mm and r = 100 mm, respectively, resulting in a beam waist radius of ω_3~40 μm at the center of the third MgO:sPPLT crystal. The stage-3 is separated by a distance of ~86.5 cm from stage-2. The MC SP-SHG is characterized using the CT oven configuration for stage-1 and stage-2, while employing the OT design for stage-3, where the nonlinear crystal is expected to suffer maximum thermal effects. The SHG efficiency scaling results at the output of each stage in the MC scheme are shown in Fig. 6(a). For this measurement, the phase-matching temperature of each of the three crystals is adjusted every time the fundamental power is increased, so as to achieve maximum overall SH green power at the output of stage-3. The input fundamental power is measured before stage-1, while the green power is measured at the output of the respective stages. The SH power in MC scheme at the output of stage-3 increases quadratically up to a fundamental power of 10 W, providing a maximum green power of 5.6 W at a maximum SHG efficiency of 56%. Further increase in the fundamental power up to 12 W results in saturation of SH power, leading to efficiency roll-off. We attribute this behavior to thermal phase-mismatch effects, back-conversion and pump-depletion. These issues are discussed in the next section. The corresponding maximum SHG efficiencies, measured at the output of stage-1 and stage-2 are 11.2% and 36.2%, respectively, which are not necessarily the maximum achievable efficiencies for the respective stages. These values at a similar fundamental power level are lower than the SHG efficiencies achieved in the SC (17.5%) and DC (42.3%) schemes. It is to be noted that the optimization procedure for SC and MC schemes is different. In case of SC scheme, we obtained maximum green power by operating the crystal at its phase-matching temperature. On the other hand, if

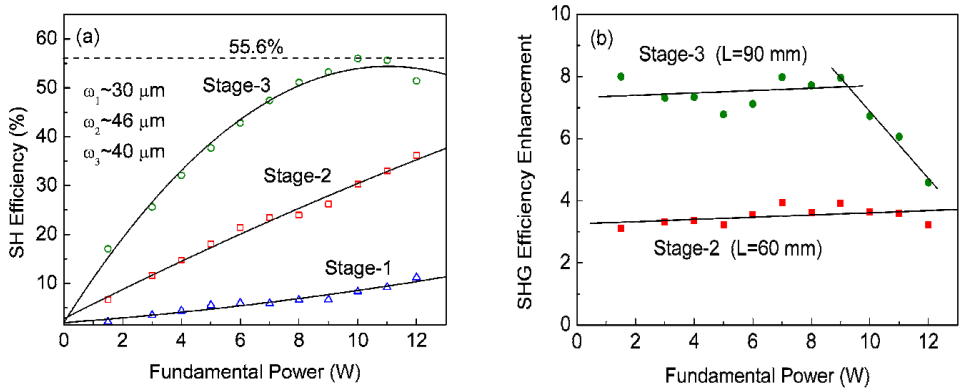

Fig. 6. Variation of (a) SHG efficiency and (b) SHG efficiency enhancement factor, as a function of fundamental power at the different stages in the MC SHG scheme for ω_1~30 μm, ω_2~46 μm, ω_3~40 μm.

#143851 - $15.00 USD Received 10 Mar 2011; revised 29 Apr 2011; accepted 17 May 2011; published 24 May 2011

we keep all the crystals at their respective phase-matching temperatures in MC scheme, the overall green power is low. This is obvious as higher depletion of the fundamental power in one stage reduces the fundamental power to get depleted in the succeeding stages thereby lowering the overall efficiency. Hence, while optimizing the MC scheme for maximum SH power at the output of stage-3, we slightly detuned the temperature of the crystals in stage-1 and stage-2 from their phase-matching temperature, as a result of which the generated green power at the output of stage-1 and stage-2 in the MC scheme is not optimum, however a clear enhancement in the overall SHG efficiency is recorded in the MC scheme, as shown in Fig. 6(a). The detuning of the phase-matching temperature in the MC scheme permits the control of pump depletion and SH power in each conversion stage, as well as the distribution of thermal load in the different crystals, resulting in maximum overall SHG efficiency and output power. This freedom also has the additional advantage of reducing the risk of optical damage in each crystal. The flexibility of controlling the phase-matching temperature in different conversion stages is one of the greatest advantages of the MC SP-SHG scheme, particularly in the high-power regime. This is the reason why perfect phase control due to the air dispersion is not required. Therefore, any slight phase shift between the fundamental and SH due to dispersion in air can be compensated by controlling the pump depletion. As the SHG efficiency scales quadratically with the length of the nonlinear crystal, an efficiency enhancement factor of 4 and 9 is expected at the output of stage-2 (L = 60 mm) and stage-3 (L = 90 mm), respectively, in comparison with stage-1(L = 30 mm). So, we also compared the SHG efficiency enhancement at the output of stage-2 and stage-3 with respect to stage-1, up to a fundamental power level of 12 W, as shown in Fig. 6(b). It can be seen that the measured SHG efficiency resulted in an enhancement of ~4 times after stage-2, as expected, while there appears to be a slight deviation after stage-3, with a recorded value of ~8 times up to a fundamental power of 9 W, above which it decreases linearly to ~4.6 times at 12 W of fundamental power. This decrease in the SHG efficiency enhancement factor is attributed to the efficiency roll-off due to thermal phase-mismatch effects, back conversion, and pump depletion.

In order to investigate the role of focusing in stage-3, we used a different set of plano-concave mirrors for M_3 and M_4, with r = 150 mm and r = 200 mm, respectively, resulting a beam waist radius of ω_3~80 µm at the center of the third MgO:sPPLT crystal. The power scaling results for the MC scheme with ω_3~80 µm in the third crystal are shown in Fig. 7, where it can be seen that loose focusing enabled pumping up to a higher fundamental power level of 17.7 W, providing a maximum SH power of 9.6 W at an efficiency of 54.3%. However, the maximum efficiency achieved still remains 55.6% at a fundamental power of 15.7 W. Hence, depending on the available pump power, the maximum SH power or the maximum efficiency can be achieved by proper choice of the focusing condition as well as length of the nonlinear crystals in the MC scheme.

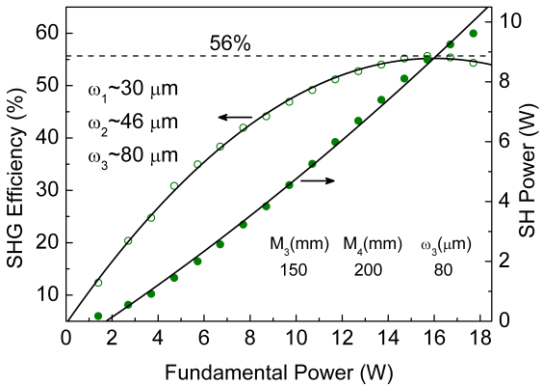

Fig. 7. Power scaling of MC SHG scheme with ω_3 ~80µm.

#143851 - $15.00 USD Received 10 Mar 2011; revised 29 Apr 2011; accepted 17 May 2011; published 24 May 2011

Further, we compare the performance of all the three schemes, with the power scaling results shown in Fig. 8(a). In the MC scheme, a maximum green power of 6.1 W is achieved for a fundamental power of 11 W at an SHG efficiency of 55.5%. The corresponding SH power generated in the SC, DC schemes are 9.6 W and 13 W, respectively. The maximum SH power generated in the MC scheme is limited by the SHG efficiency roll-off. Importantly SHG efficiency as high as 56% is achieved for a fundamental power as low as 10 W in the MC scheme, while achieving a SHG efficiency of 54.8% in the DC scheme requires 21.1 W of fundamental power, as evident in Fig. 8(b). These values of the required fundamental power are in close agreement with the theoretical estimates made from Fig. 2. Clearly, the required fundamental power to achieve similar maximum SHG efficiency reduces by ~2 times (or 50%) in the MC scheme as compared to DC scheme, while such efficiency could not be achieved in the SC scheme using a single 30-mm-long MgO:sPPLT crystal with the available 30 W fundamental power, as evident from Fig. 8(b). The corresponding low-power normalized conversion efficiencies are 1.4%/W, 5%/W and 7.8%/W for the SC, DC and MC scheme, respectively.

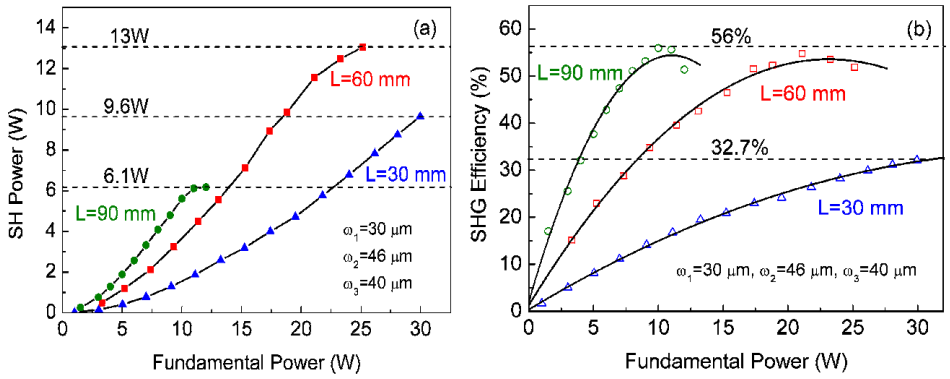

Fig. 8. Comparison of (a) SH power scaling, and (b) SHG efficiency in SC, DC, and MC schemes.

2.6 Effect of dispersion in air

In order to study the effect of the inter-crystal spacing on the SHG efficiency enhancement because of the phase accumulation between the fundamental and the SH, due to dispersion in air in the DC scheme, we used the formalism developed in Ref. [27]. Any additional phase accumulation due to the mirrors is also accounted for. Considering an experimentally measured SH efficiency enhancement factor of 3.8 for a separation of 37 cm between the two stages in DC scheme, we estimated a relative phase accumulation of $\Delta\varphi = 17.4$ radians due to the mirrors. With this estimate of $\Delta\varphi$, we investigated the effect of inter-crystal spacing on the SHG efficiency. The calculated variation of the SHG efficiency enhancement factor as a function of inter-crystal spacing in a DC scheme is shown in Fig. 9. For this calculation, we used a linear absorption coefficient of 0.17%/cm, 1.57%/cm for MgO:sPPLT crystal at the fundamental and the SH wavelengths respectively, as measured in our previous experiments [15]. The phase shift of 27.4°/cm between the fundamental and the SH waves due to dispersion in air is assumed. As evident from Fig. 9, a considerable change in the SHG efficiency enhancement requires the distance between the crystals to be varied by few centimeters. The vertical dashed line in Fig. 9 represents the SHG efficiency enhancement for a distance of 37 cm between the crystals, which we have used in the present experiment for DC scheme. This distance is very close to the optimum distance which can provide a theoretical maximum SHG efficiency enhancement.

#143851 - $15.00 USD Received 10 Mar 2011; revised 29 Apr 2011; accepted 17 May 2011; published 24 May 2011

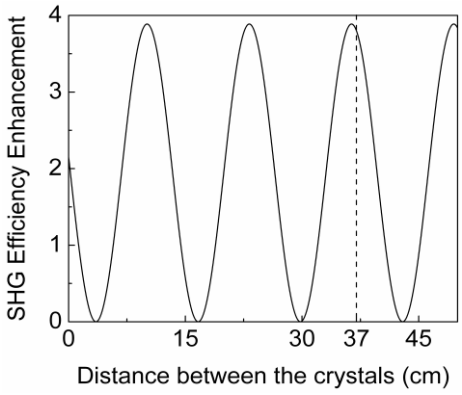

Fig. 9. Theoretically calculated variation of the SHG efficiency enhancement factor as a function of the distance between the crystals in DC scheme for $\Delta\varphi = 17.4$ radians.

2.6. Thermal effects and SHG efficiency roll-off

In order to study the role of thermal effects in the MC cw SP-SHG scheme, we performed temperature tuning measurements in stage-3, where the heaviest thermal load is expected due to the highest SH power, since the residual absorption of the crystal is ~9 times higher at 532 nm than at 1064 nm [15]. While performing these measurements, stage-1 and stage-2 are optimized for maximum SH power. The dependence of the normalized SH power on the temperature of the nonlinear crystal in stage-3 at a fundamental power of 11 W is shown in Fig. 10(a). It is to be noted that a non-zero SH power is measured even when the stage-3 is completely out of phase-matching because of the contribution from stage-1 and stage-2. The solid curve is the $sinc^2$ fit to the data, which has a full-width at half maximum (FWHM) bandwidth of $\Delta T = 1.3$ °C at a phase-matching temperature of 50.9 °C. This is slightly wider than the theoretically calculated value of $\Delta T = 0.96$ °C for a 30-mm-long MgO:sPPLT crystal using the Sellmeier equations for the material [34]. The temperature acceptance bandwidth is similar to that measured in the SC scheme [15,16]. The discrepancy between the calculated and measured temperature acceptance bandwidth values arises from various factors including focusing, possible non-uniformity of the grating period, and thermal effects [15]. A wider temperature acceptance bandwidth is anticipated for SHG process, because it indicates that the generated SH power is less susceptible to minor temperature fluctuations about the phase-matching temperature. As the temperature acceptance bandwidth is inversely proportional to the length of the nonlinear crystal, employing single 90-mm-long MgO:sPPLT crystal would

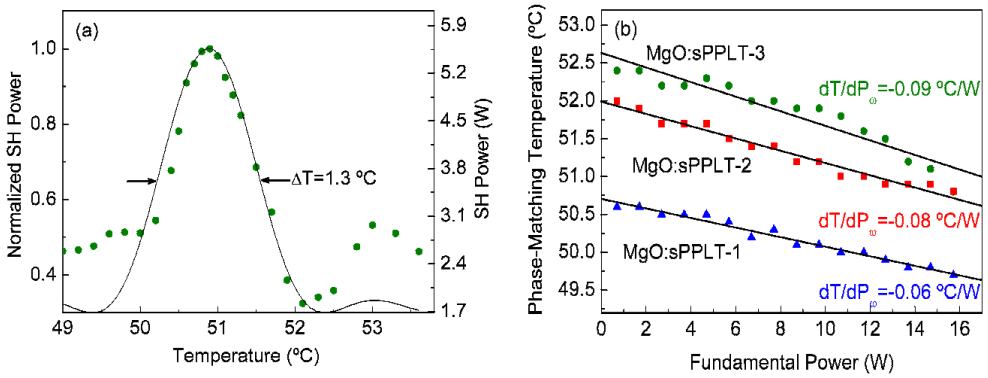

Fig. 10. (a) Temperature acceptance bandwidth of the third crystal, and (b) Change in phase-matching temperature as a function of fundamental power in SC, DC and MC schemes.

#143851 - $15.00 USD Received 10 Mar 2011; revised 29 Apr 2011; accepted 17 May 2011; published 24 May 2011

result in a ΔT = 0.32 °C, which is 3 times lower than that for a 30-mm-long crystal. However, by deploying the MC SHG scheme, we can exploit the advantage of a much longer total interaction length, but without incurring the penalty for a reduced temperature acceptance bandwidth. This would also be true for spectral acceptance bandwidth. Additionally, since the beam focusing condition in the MC scheme can be independently controlled for each stage, one can achieve a similar angular acceptance bandwidth for the total number of crystals in the cascade as for a single crystal.

The rate of change of phase-matching temperature with respect to fundamental power up to 16 W, in all the three schemes, is shown in Fig. 10(b). The phase-matching temperature in SC scheme decreases from 50.6 °C to 49.7 °C at a rate of 0.06 °C/W. In the DC scheme, while the phase-matching temperature of the nonlinear crystal in stage-1 is optimized for maximum SH power, the phase-matching temperature of stage-2 decreases from 52 °C to 50.8 °C at a rate of 0.08 °C/W. Similarly, with the phase-matching temperature of stage-1 and stage-2 optimized for maximum SH power, the phase-matching temperature of stage-3 in MC scheme decreases from 52.4 °C to 50.8 °C at a rate of 0.09 °C/W. This value in the MC SHG scheme is similar to that of PPKTP in the SC scheme, also measured up to a fundamental power level of 16.4 W [15], indicating the superior performance of MgO:sPPLT due to its high thermal conductivity. Further, owing to the fact that the absorption coefficient of MgO:sPPLT crystal at 532 nm (1.57%/cm) is ~9 times higher than that at 1064 nm (0.17%/cm), it is expected that the crystal in the third stage is prone to the heaviest thermal load. However, as the length of the nonlinear crystal increases, which in the present case is achieved by using multiple crystals, the amount of fundamental power required to attain the maximum SHG efficiency before the onset of any roll-off decreases rapidly, not only reducing the thermal effects due to absorption of fundamental by 3 times in the MC scheme as compared to SC scheme, but also distributes the thermal load due to the SH wavelength in all three stages. This thermal management can be seen as one of the main advantages of the MC scheme, which is very difficult in a single long crystal, in addition to the possibility of achieving high SHG efficiencies.

In order to verify the contribution of thermal effects to SHG efficiency roll-off, we chopped the fundamental beam at a frequency of 510 Hz, with a 5.1% duty cycle, and performed power scaling measurements in DC and MC schemes, separately. The quasi-cw SH power and efficiency scaling results are shown in Fig. 11(a)-(b). The generated average SH power in DC scheme reaches a maximum of 0.6 W for an average fundamental power of 1.3 W at a SH efficiency of 48.9% as can be seen from Fig. 11(a). Similar measurement for pure cw pumping resulted in a SH efficiency of 54.8%, as shown in Fig. 5(b). In MC scheme, a maximum average SH power of 0.4 W is generated for an average fundamental power of 0.7 W at a SHG efficiency of 55%, above which SH power saturation and efficiency roll-off sets in, as evident from Fig. 11(b). The maximum SHG efficiency achieved by quasi-cw pumping

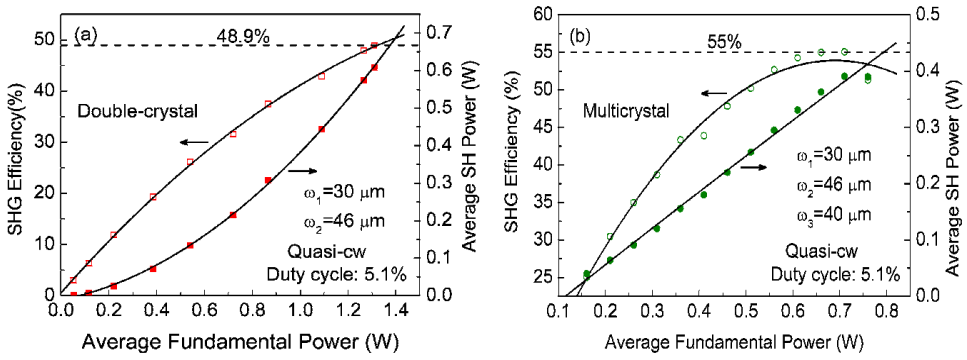

Fig. 11. Quasi-cw power scaling of (a) double-crystal, and (b) multicrystal schemes.

#143851 - $15.00 USD Received 10 Mar 2011; revised 29 Apr 2011; accepted 17 May 2011; published 24 May 2011

is similar to that achieved by pure cw pumping (56%, as shown in Fig. 8(b)), indicating minimal contribution of thermal effects to SHG efficiency roll-off in MC scheme, leaving pump depletion as a possible reason.

2.7 Power stability and output beam quality

In order to completely characterize the MC cw SP-SHG scheme, we have measured the power stability and beam quality of the SH beam at the output of stage-3. The power stability of the SH output beam is influenced by various factors such as power stability of the fundamental, fluctuations in the temperature of the nonlinear crystal, air currents and mechanical vibrations in the laboratory environment. The power stability of the Yb fiber laser fundamental beam is measured to be better than 1% over 65 minutes and the SH beam at the output of the SC scheme was measured as 9% over 13 hours in our earlier report [16]. This stability is now improved to better than 2.2% over one hour, as shown in Fig. 12(a), which has been achieved by using a more uniform heating configuration for the MgO:sPPLT crystal, where the 30-mm crystal is placed at the center of a large-area oven for heating. As compared to the small-area oven used previously [15,16], the central part of the large-area oven has better temperature uniformity and is less sensitive to the instability (± 0.1°C) determined by the temperature controller. As a result, the large-area oven maintains improved temperature stability across the full length of the crystal, and hence a better green output power stability. Due to the limited availability of large-area ovens in our laboratory, they are only deployed in stage-1 and stage-2 of the MC SHG scheme, while stage-3 uses a small-area oven. Figure 12(b) shows the green power stability measurement at the output of MC scheme at a SH power of 5.5 W and a SHG efficiency of 55%, resulting in a peak-to-peak fluctuation of 6.5% over > 2 hours. We have also recorded long-term peak-to-peak power stability better than 10.5% over 10 hours. Further improvement in the SH power stability is possible by incorporating the entire MC SHG setup in a mono-block, thereby minimizing the influence of air currents and mechanical vibrations.

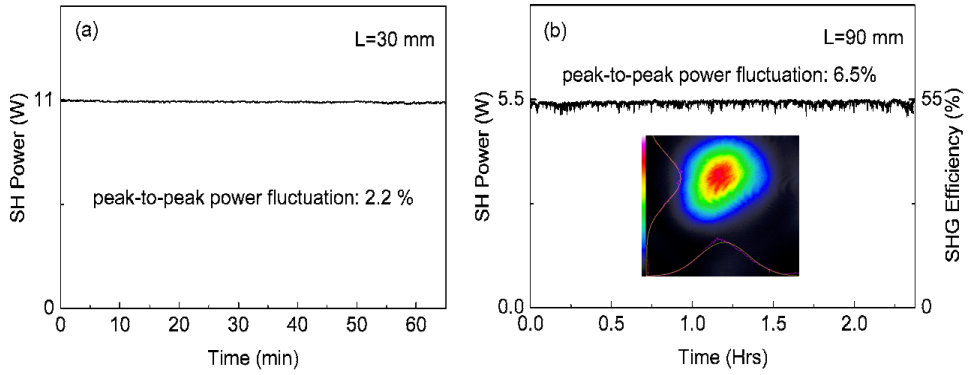

Fig. 12. Second harmonic power stability at the output of (a) SC and (b) MC scheme.

Further, we have also characterized the SH beam quality at the output of the MC SP-SHG setup. The inset of Fig. 12(b) shows the far-field energy distribution of the SH green beam, as measured at an incident fundamental power of 11 W and maximum SHG efficiency, together with the horizontal and vertical intensity profiles confirming a Gaussian beam profile. The slight asymmetry in the beam profile may be attributed to the number of plano-concave mirrors used at a small angle away from normal incidence in the MC scheme, and so could be overcome by further design improvements to reduce the angles of incidence on the focusing mirrors. Using a scanning beam profiler and a f = 20 cm focal length lens, we measured the beam diameter over the Rayleigh range of the focused SH beam at the output of the MC SHG setup, and determined the corresponding M^2 values in the horizontal and vertical directions. This measurement was performed at a SHG efficiency of 55% and resulted in a value of M_x^2~1.6 and M_y^2~1.34. These values are comparable to M_x^2~1.6 and M_y^2~1.52 measured in the

#143851 - $15.00 USD Received 10 Mar 2011; revised 29 Apr 2011; accepted 17 May 2011; published 24 May 2011

DC scheme at a SHG efficiency of 50%, and M_x^2~1.29 and M_y^2~1.23 in the SC scheme at a SHG efficiency of 32.7% [15,16], confirming TEM_{00} spatial mode in the MC scheme.

3. Conclusions

In conclusion, we have presented detailed studies of a novel multicrystal scheme for efficient SP-SHG of cw laser radiation. Using a cw Yb fiber laser in combination with three MgO:sPPLT nonlinear crystals, record cw SHG efficiencies as high as 54.8% and 56% into the green have been achieved, for fundamental powers of 21.1 W and 10 W, in DC and MC schemes, respectively, and the efficiencies have been found to be in close agreement with the theoretical estimates. The optimization of various vital parameters including focusing and phase-matching temperature at the output of each individual stage to maximize the SHG efficiency has been investigated. The SC, DC and MC SHG schemes have been systematically characterized and their results are compared, as summarized in Table 2. By employing different oven designs, the OT configuration enabled pumping at high fundamental power levels, thus permitting higher SHG efficiencies. We have observed SHG efficiency roll-off in DC and MC schemes, irrespective of the oven design and focusing conditions. In the MC scheme, although the maximum SHG efficiency achieved is similar (56%), loose focusing in the third crystal (ω_3~80 μm) not only postponed the SHG efficiency roll-off, but also allowed pumping to a higher fundamental power of 17.7 W, resulting in a maximum SH power as high as 9.6 W, while focusing to ω_3~40 μm resulted in a SH power of 6.1 W only at a fundamental power of 11 W. We have also recorded a SHG efficiency enhancement factor of ~4 and ~8 up to a fundamental power of 12 W and 9 W in stage-2 and stage-3 of MC scheme, respectively. The effect of dispersion between the fundamental and the SH beams in air has been estimated with relevant theoretical calculations, indicating that a substantial change in the SHG efficiency enhancement factor requires variation of the distance between the successive crystals on the order of a few centimeters.

Table 2. Summary of multicrystal, single-pass SHG results

	Scheme		
	SC	DC	MC
Crystal length (mm)	30	60	90
Beam waist (μm)	ω_1~30	ω_1~30 ω_2~46	ω_1~30 ω_2~46 ω_3~80
Oven configuration	OT	CT-OT	CT-CT-OT
Highest SHG conversion efficiency (%)	32.7	54.8	56
Low power normalized SH conversion efficiency (%/W)	1.4	5	7.8
M^2 value	<1.29	<1.6	<1.6

Studies of thermal effects have included measurements of temperature acceptance bandwidth and rate of change of phase-matching temperature with fundamental power. Quasi-cw SHG studies have confirmed minimal contribution of thermal effects to SHG efficiency roll-off in the MC scheme. Further, we have improved the peak-to-peak SH power stability of SC scheme to better than 2.2% over an hour, since our earlier report, by employing large-area oven for uniform heating of the nonlinear crystal and the peak-to-peak SH power stability in MC scheme is recorded to be better than 6.5% over more than 2 hours and a long term stability better than 10.5% over 10 hours. This performance has been achieved in high spatial beam quality with M_x^2~1.6 and M_y^2~1.34, as compared to M_x^2~1.6 and M_y^2~1.52 in a DC scheme, and M_x^2~1.29 and M_y^2~1.23 in SC scheme, confirming TEM_{00} mode profile. Further improvement in the stability and spatial beam quality are possible with proper design and optimization without any effect on SH power and efficiency. The generic nature of the multicrystal scheme described here offers a simple yet effective technique for the attainment

#143851 - $15.00 USD Received 10 Mar 2011; revised 29 Apr 2011; accepted 17 May 2011; published 24 May 2011

of maximum SHG efficiency and output power in SP-SHG of cw laser radiation at other wavelengths and over a wide range of fundamental powers.

Acknowledgments

This research was supported by the Ministry of Education and Science, Spain, through grant TEC2009-07991 and the Consolider project, SAUUL (CSD2007-00013). We also acknowledge partial support of this research by the Seventh Framework Program of the European Union—MIRSURG (224042) and the European Office of Aerospace Research and Development (EOARD) through grant FA8655-09-1-3017.

#143851 - $15.00 USD Received 10 Mar 2011; revised 29 Apr 2011; accepted 17 May 2011; published 24 May 2011